Isothermal aggregation of Ag atoms in sodium borate glass

G. Kellermann[1,*] and A. F. Craievich[2]
[1]*Laboratório Nacional de Luz Síncrotron, C. P. 6192, 13084-971 Campinas SP, Brazil*
[2]*Instituto de Física, USP, C.P 66318, CEP 05315-970, São Paulo SP, Brazil*
(Received 11 December 2003; revised manuscript received 1 April 2004; published 26 August 2004; publisher error corrected 3 September 2004)

The nucleation and growth of Ag nanocrystals, embedded in an initially homogeneous and supersaturated Ag-doped sodium borate glass, were studied by *in situ* small-angle x-ray scattering (SAXS) during isothermal annealing at different temperatures, from 813 up to 843 K. The SAXS results corresponding to the as-quenched glass indicate that some amount of rather large Ag nanocrystals are formed during the fast cooling stage. After a few minutes, the formation and growth of another population of small Ag nanocrystals occur. The formation of this fine nanocrystalline phase exhibits two distinct stages after a short incubation period. Initially, Ag clusters grow as a consequence of the "up-hill" diffusion of individual Ag atoms through the glass matrix and further aggregation and, at a more advanced stage, by the coarsening of the Ag nanocrystals formed in the preceding stage. The time dependences of the experimental functions describing the average radius, relative size dispersion, and density number of nanocrystals during the advanced stages of growth, all agree with the predictions of the classical Lifshitz-Slyozov-Wagner (LSW) theory. However, the nanocrystal radius distribution is well described by a log-normal function, which leads to a fit of the modeled scattering intensity to the experimental curves better than the function predicted by the classical LSW model. From the SAXS results at different annealing temperatures the activation energy involved in the Ag diffusion through the glass matrix was inferred.

DOI: 10.1103/PhysRevB.70.054106 PACS number(s): 61.10.Eq, 66.10.Cb, 81.10.Jt

I. INTRODUCTION

The investigation of the structure and properties of nanometer sized metallic particles have attracted the interest of many scientists because of their possible use in catalysis and in other technological fields. Due to their singular optical properties and potential application in nanoscale electronic devices, particular attention is currently being addressed to nanostructured materials consisting of metallic nanoclusters embedded in glass matrices. Optical properties of glass-metallic nanocluster composites, in general, strongly depend on the average cluster size and, often, a narrow size dispersion is a necessary condition for practical utilization. A review of the optical properties of these materials and of the methods used in their preparation and characterization were reported by Gonella and Mazzoldi.[1]

This is an investigation of the kinetic of formation and growth of Ag nanocrystals embedded in a sodium borate glass. Supersaturated Ag-doped glasses were studied by *in situ* small-angle x-ray scattering (SAXS) during isothermal annealing at different temperatures between 813 and 843 K, these temperatures being higher than that corresponding to the sodium borate glass transition $T_g = 758$ K (Ref. 2). The basic purpose was to obtain, from the results of SAXS experiments, the time-dependent radius distribution and, from it, the time dependence of the average radius, radius dispersion, number density, and total volume fraction. Finally, the experimental results were critically compared with the predictions of the classical theories for cluster growth.

II. EXPERIMENT

The starting raw materials were Na_2CO_3, B_2O_3, $AgNO_3$, and SnO. SnO was added as a reducing agent for Ag_2O. To avoid oxidation of SnO by air, the mixture was melted in an electrical furnace under vacuum (10^{-1} mbar) at 1313 K. A $28Na_2O$-$72B_2O_3$ (mol %) glass containing dispersed Ag atoms was obtained by fast quenching of the melted glass down to room temperature using the splat-cooling technique. The resulting 100–150 μm thick glass plates were homogeneous and transparent to visible light. Apart from producing thin glass plates, ready for SAXS experiments, the fast splat-cooling procedure is particularly efficient because it prevents glass crystallization and suppresses, or strongly reduces, the formation of Ag clusters during cooling. The SAXS intensity produced by the glass samples was measured *in situ*, during isothermal annealing at temperatures ranging from 813 up to 843 K inside a high temperature cell.[3] During the annealing cycles, the glass plates became slightly yellow thus evidencing the expected variation in optical absorption associated to the formation of metallic nanocrystals.

The *in situ* SAXS experiments were performed using the SAXS beamline of the Brazilian Synchrotron Light Laboratory (LNLS), Campinas, Brazil.[4] A one-dimension gas x-ray position-sensitive detector was used to measure the SAXS intensity as a function of the scattering angle for different increasing periods of time. The attenuation of the studied samples was determined using two scintillation detectors, which monitored the intensities of the direct and transmitted x-ray beams. The SAXS spectra were normalized to equivalent intensity of the direct beam in order to compensate for the continuous decrease in intensity of the x-ray beam emitted by the synchrotron source. The experimental SAXS intensity was determined as a function of the modulus of the scattering vector, $q = 4\pi \sin\theta/\lambda$, where λ is the wavelength of the x-ray beam ($\lambda = 1.61$ Å) and θ is half the scattering

angle. The parasitic scattering produced by slits was subtracted from the total SAXS intensity. Because of the small area of the cross section of the transmitted x-ray beam at the detection plane and the narrow resolution slit of the x-ray detector, the SAXS curves were essentially free from smearing effects. In order to determine the scattering power of the studied samples (i.e., the scattering intensity in absolute units), the SAXS intensity produced by water was also measured under the same collimation condition.[5]

III. CLASSICAL THEORY OF COARSENING

The formation and growth of a new phase consisting of nanoclusters embedded in an initially homogeneous and supersaturated matrix begin with a nucleation stage and is followed by the growth of the nuclei promoted by the up-hill diffusion of doping atoms. This mechanism is named "nucleation and growth". After this initial stage, the clusters embedded in a homogeneous matrix coarsen. For long annealing times, when the supersaturation of the doping element in the matrix become low, clusters with a radius R smaller than a critical radius R_c start to dissolve while those with radii larger than R_c still grow. The coarsening of a dilute set of spherical clusters—each one located far away one from the others—is described by the model proposed by Lifshitz-Slyosov[6] and Wagner[7] (LSW model). The driven force for coarsening is associated to the overall decrease in interface area between clusters and matrix, thus reducing the total interface energy. According to LSW model, in absence of significant elastic stresses, the cluster radius distribution $N(R,t)$, for long annealing times, does not depend on the initial size distribution $N(R,0)$ and is given by:[6]

$$N(R,t) = f(t)\frac{4(R/R_c)^2}{9}\left(\frac{3}{3+R/R_c}\right)^{7/3}\left(\frac{3/2}{3/2-R/R_c}\right)^{11/3} \times \exp\left(\frac{-R/R_c}{3/2-R/R_c}\right), \quad (1)$$

where $f(t)$ is a function of the annealing time only. Under the assumptions of the LSW model R_c coincides with the average cluster radius $\langle R\rangle$. The LSW theory predicts the time dependences of the clusters average radius $\langle R\rangle(t)$, the concentration of solute atoms in the matrix $c(t)$ and the total number density of clusters $n(t)=\int N(R,t)dR$.

During the coarsening stage, $\langle R\rangle(t)$ increases for increasing times while $n(t)$ progressively decreases. Quantitatively, according to the LSW model, after the initial time for coarsening t_0, the time dependence of $\langle R\rangle(t)$, $n(t)$, and $c(t)$ satisfies the following equations:[6–8]

$$\langle R\rangle^3(t) = \langle R_0\rangle^3 + \frac{8\gamma\nu^2 c_e D}{9kT}(t-t_0), \quad (2)$$

$$n^{-1}(t) = n_0^{-1} + \frac{4\gamma c_e \nu D}{(c_i - c_e)kT}(t-t_0), \quad (3)$$

$$c(t) = c_e + \left[\frac{D(kT)^2}{9\gamma^2 c_e^2 \nu}\right]^{-1/3}(t-t_0)^{-1/3}, \quad (4)$$

where $\langle R_0\rangle$ and n_0 are the average radius and number density of the nanoclusters, respectively, at the starting time for coarsening $t=t_0$, c_e is the concentration of solute atoms in the matrix at equilibrium, D the atomic diffusion coefficient of the solute atoms, γ the free energy per unit of area of the interface between clusters and matrix, ν the atomic volume of the solute, c_i the initial concentration of solute in the matrix, k the Boltzmann constant, and T the absolute temperature.

An equation equivalent to (4) can be written in terms of the volume fraction of the new phase:[9]

$$\varphi(t) = \varphi_e - \left(\frac{1-\varphi_e}{\nu^{-1}-c_e}\right)\left[\frac{D(kT)^2(t-t_0)}{9\gamma^2 c_e^2 \nu}\right]^{-1/3}, \quad (5)$$

where φ_e is the volume fraction of the new phase at equilibrium. Equations (2)–(5) hold for annealing times $t \geqslant t_0$.

The relative radius dispersion determined from Eq. (1) $\sigma_R = \sigma/\langle R\rangle$, where σ is the standard deviation of the clusters radius distribution, is time independent and equal to 0.21. This is a consequence of the dynamical self-similarity of the structure during the cluster coarsening predicted by the LSW theory.

The LSW model applies to *dilute* two-phase systems composed of spherical clusters occupying a small fraction of the total volume (i.e., the infinitely diluted limit). As it was demonstrated in previous works,[10–12] the finite volume fraction of the minor phase has a modifying effect on the coarsening kinetics leading to changes in the rate constant as well as in the shape of the radius distribution function. Deviation from the basic LSW model can also be produced by elastic strains in the matrix near the growing cluster. These strains may modify the kinetic of cluster growth and eventually the total coarsening process.[8,13]

IV. RESULTS AND DISCUSSION

The aim of this study is to characterize the mechanisms of formation and growth of a dilute and isotropic set of Ag nanocrystals embedded in an initially homogeneous and Ag supersaturated sodium borate glass. The study was performed using the SAXS technique *in situ* during isothermal annealing of the samples at different temperatures.

Figure 1 exhibits the experimental SAXS intensity functions corresponding to different periods of thermal annealing at 813 K. The fast increase in the SAXS intensity, from the very beginning of isothermal treatment, suggests that Ag-rich nuclei already exist in the initial glass, these clusters being developed during the quenching. After the first 300 s of annealing, the time evolution of the SAXS intensity profiles indicates the formation and growth of a second population of small Ag precipitates. The analysis of the SAXS curves during the early stages of isothermal annealing indicates a very fast increase in the average radius of the Ag nanocrystals already present in the initial glass. Guinier plots[14] over the very low q range indicate that these Ag clus-

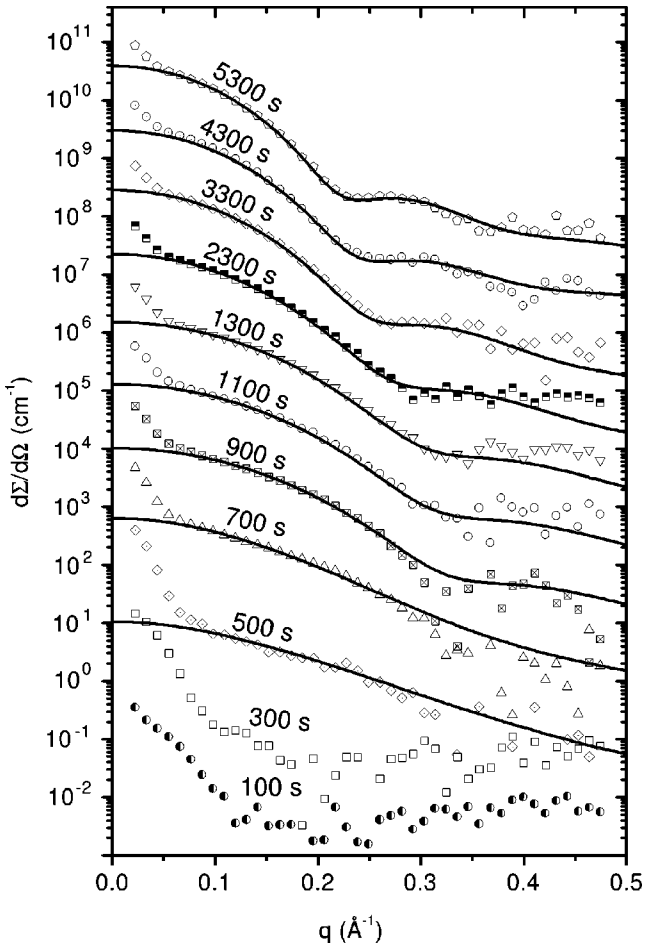

FIG. 1. The curves with symbols are the SAXS intensities in absolute units produced by the Ag doped glass annealed at 813 K during the indicated time periods. The solid lines are the modeled scattering intensities determined by a standard best-fit procedure assuming log-normal radius distribution functions. For clarity the curves from 300 through 5300 s are multiplied by successively increasing powers of 10.

ters have an average radius equal to 57 Å for $t=300$ s. Because of limitations in the experimentally accessible minimum q value, a more detailed analysis of the large sized Ag nanocrystals population was not performed. Instead, we have focused our investigation to the kinetic of growth of the small-sized nanocrystals population formed during the further isothermal annealing process. The contribution to the SAXS intensity from the large nanocrystals overlaps the intensity of the second family of small nanocrystals only within a short range at very small q. Thus, this small portion of the scattering curve was not considered in our further analysis.

The lack of evidence for the formation of a second Ag nanocrystals population up to 300 s of annealing at 813 K (see Fig. 1) implies the existence of an incubation time for nanocrystals nucleation. The same qualitative behavior was also observed for glasses annealed at 823 and 843 K. Our experimental results indicate that the incubation time decreases for increasing temperatures, this being an expected consequence of the strong increase of the diffusion coefficient for rising temperatures.[15]

A previous study of Ag nanocrystals embedded in the same glass using transmission electron microscopy (TEM) demonstrated that nanocrystals are homogeneously dispersed in the glass and have nearly spherical shape.[2] In the same article it was demonstrated that the Ag nanocrystals have a cubic close-packed structure like in bulk state.

The scattering intensity in absolute units, i.e., the x-ray scattering power, is usually written as a differential scattering cross section $d\Sigma/d\Omega$. For a dilute set of uncorrelated spherical nanocrystals with constant electron density ρ_p embedded in an homogeneous medium with a constant electron density $\langle\rho\rangle$, the scattering power is given by:[14]

$$\frac{d\Sigma}{d\Omega}(q) = r_0^2(\Delta\rho)^2\left(\frac{4\pi}{3}\right)^2\int_0^\infty N(R)P(q,R)R^6\,dR, \qquad (6)$$

where $r_0=0.28179\times10^{-14}$ m is the classical electron radius, $N(R)dR$ is the number of nanocrystals per unit volume with radius between R and $R+dR$, $\Delta\rho=(\rho_p-\langle\rho\rangle)$, and $P(q,R)$ is the normalized form factor for a sphere defined by

$$P(q,R) = \left[3\frac{\sin(qR)-qR\,\cos(qR)}{(qR)^3}\right]^2. \qquad (7)$$

The same glass without Ag atoms exhibits an essentially q independent contribution to the scattering intensity. This constant background, produced by statistical electron density fluctuations in the glass matrix, was experimentally determined for the studied samples by using Porod plots[14] and then subtracted from the total scattering intensity.

According to the previous TEM study mentioned above,[2] the implicit assumption of our model, regarding the dilute nature of the solution and the spherical shape of the clusters, applies to the system that we study here. The electron densities of the glass matrix $\langle\rho\rangle$ and of Ag nanocrystals ρ_p were determined from the known nominal composition and mass density of the glass and from the crystalline structure of bulk Ag, respectively. Due to the continuous decrease in the concentration of Ag atoms dissolved in the glass matrix, a variation in the difference between the electron density of Ag nanocrystals and the glass matrix $(\Delta\rho)$ is expected. Due to the small concentration of Ag atoms in the glass, this difference is only very slightly modified during the whole annealing process and thus was assumed to be a time constant.

The experimental x-ray scattering power corresponding to advanced stages of thermal annealing was modeled assuming the radius distribution predicted by LSW theory, Eq. (1). However, the fit of Eq. (6) to the experimental SAXS results assuming $N(R)$ given by Eq. (1) is not good. On the other hand, a better fit to the experimental curves was obtained using the log-normal function defined as

$$N(R) = \frac{n}{\sqrt{2\pi\,\exp(b^2)}\,b\,a}\exp\left\{-\frac{1}{2}\frac{[\ln(R/a)]^2}{b^2}\right\}. \qquad (8)$$

In the equation described above, a and b are fitting parameters and n is the nanocrystal number density.

The scattering power corresponding to samples annealed during 5300 s at different temperatures and the best modeled curves [Eq. (6)] for the LSW and log-normal size distribution

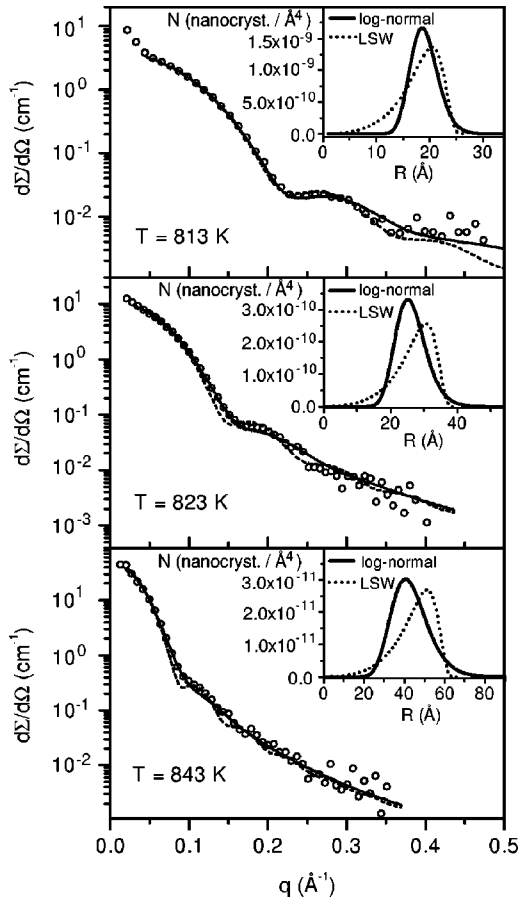

FIG. 2. Experimental scattering intensities (symbols) corresponding to the samples annealed during 5300 s at the indicated temperatures and modeled scattering curves [Eq. (6)] using the LSW (dashed lines) and log-normal (continuous lines) size distribution functions [Eqs. (1) and (8), respectively]. The $N(R)$ curves determined from the fitting procedure are plotted in the insets.

functions [Eqs. (1) and (8)] are plotted in Fig. 2. The radius distribution functions determined from the best-fit procedure assuming both functions are plotted in the insets of Fig. 2. The integral parameters [$\langle R\rangle(t)$, $n(t)$, and $\varphi(t)$] were determined as functions of time. In spite of the difference in the shape of $N(R)$, no significant discrepancies in the calculations of the integral parameters were observed. This implies that the relevant structural parameters commonly used to characterize the mechanism of growth, $\langle R\rangle(t)$, $n(t)$, and $\varphi(t)$, are not very sensitive to the detailed shape of the $N(R)$ function.

As mentioned in the preceding section, deviations of $N(R)$ from the function predicted by LSW theory were already observed by a number of previous authors.[10–13] In particular log-normal size distribution functions were established for the coarsening of semiconductor nanocrystals embedded in a glass matrix[16] and for metal clusters in a metallic matrix.[17] In a previous study of the coarsening of Bi nanodroplets in sodium borate glass,[18] it was also demonstrated that the log-normal function yields a good fit of the modeled scattering functions to the experimental SAXS curves. In these cited works (Refs. 16–18) the physical reasons for the deviation of $N(R)$ from the radius dependence expected by the LSW theory for coarsening were not discussed. Also no alternative model that could explain the deviations here observed was found in the literature. To our knowledge there is not an evident connection between a particular property of these systems and the features of the observed log-normal size distribution function. In this way, efforts toward the development of an adequate theoretical description have to be performed. However, as it will be seen in further data analysis, in spite of the discrepancy regarding the shape of the radius distribution, the time dependences of $\langle R\rangle(t)$, $n(t)$, and $\varphi(t)$ behaves as predicted by LSW theory.

The log-normal radius distributions $N(R,t)$ associated to the modeled scattering power curves corresponding to different annealing times at 813 K are plotted in Fig. 3. After the initial nucleation period, we observe a continuous growth of the average radius and a progressive reduction in the number of nanocrystals, evidenced by a shift of the maximum of the distribution toward higher R 's and by the reduction of the area under the $N(R,t)$ curves, respectively. From the $N(R,t)$ function obtained by the described fitting procedure applied to the whole set of scattering curves, the time variations of the nanocrystals average radius $\langle R\rangle(t)$, number density $n(t)$,

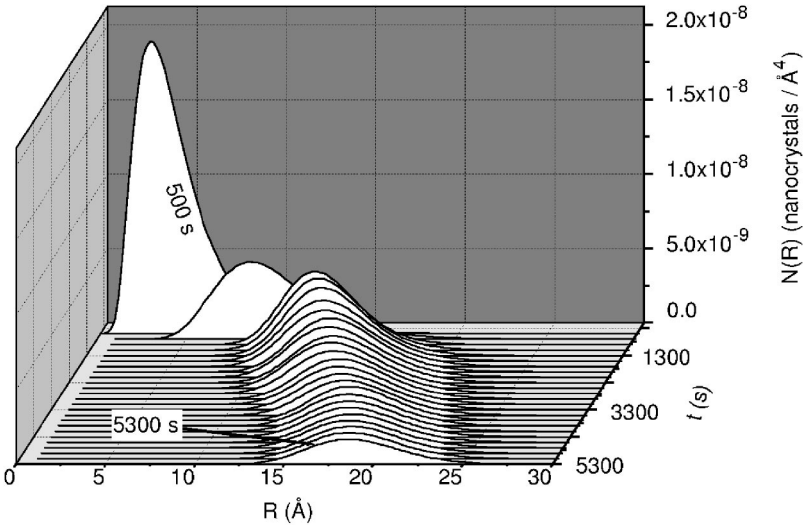

FIG. 3. Radius distribution functions $N(R,t)$ of Ag nanocrystals for different annealing times at 813 K determined from SAXS results.

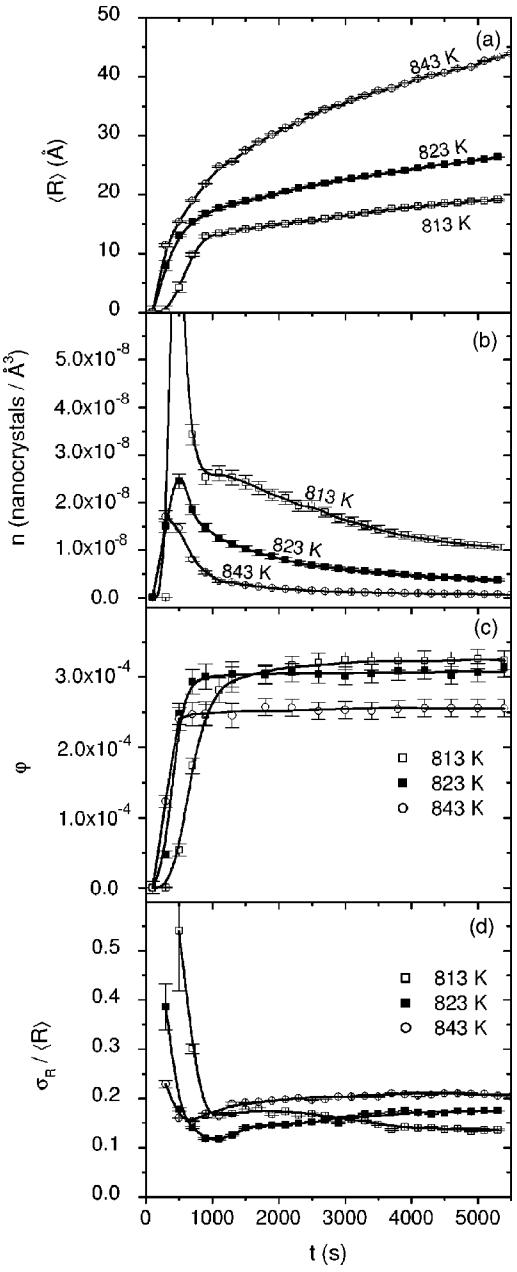

FIG. 4. Time dependences of (a) average radius $\langle R\rangle$, (b) number per unity volume n, (c) fraction of the total volume φ, and (d) relative size dispersion σ_R, of Ag nanocrystals corresponding to the population formed during isothermal annealing.

fraction of the total volume $\varphi(t)$, and relative radius dispersion $\sigma_R(t)$ were determined.

Figure 4(a) displays the time dependence of $\langle R\rangle$ for different annealing temperatures. After an initial induction period, a very fast growth of nanocrystals is observed. Later, nanocrystals grow at a lower rate until the end of the annealing process is reached. For equivalent annealing times, $\langle R\rangle$ is an increasing function of the annealing temperature. This is the expected consequence of the strong temperature dependence of the atomic diffusion coefficient. After 5300 s of annealing, Ag nanocrystals have a size distribution function with an average radius equal to 19 and 43 Å for annealing temperatures of 813 and 843 K, respectively.

The nanocrystals number density, $n(t)$, is plotted in Fig. 4(b). The fast increase observed for short annealing times corresponds to the "nucleation and growth" stage. This period is followed by a stage during which a continuous reduction in $n(t)$ occurs. At this stage, the rate of reduction in the number density is a decreasing function of time.

Fig. 4(c) displays the time dependence of the fraction of the total volume $\varphi(t)$ occupied by the Ag nanocrystals. The fast increase observed in the first period of annealing indicates that nanocrystals grow mainly by the incorporation of Ag atoms initially dissolved in the glass matrix. After this period, φ still increases but at much lower rate.

In order to verify the validity of the predictions of the LSW theory for coarsening regarding the time dependence of $\langle R\rangle$ and n [Eqs. (2) and (3), respectively], different graphical procedures are commonly used. One of them, which uses plots of $\log(\langle R\rangle)$ and $\log(n)$ versus $\log(t)$, has often been applied.[19,20] For long annealing times, for which $\langle R\rangle(t) \gg \langle R_0\rangle$ and $n(t) \ll n_0$, the log-log plots are expected to asymptotically yield straight lines with slopes 3 and −1, respectively. An alternative procedure, also applied in previous works,[21,22] consists of plotting $\langle R\rangle^3(t)\times t$ and $1/n(t)\times t$. Good fits of these experimental functions to straight lines, from the beginning until the end of the coarsening stage, also demonstrate that Eqs. (2) and (3) hold. We have preferred this second procedure because in our case the simple linear behavior is expected to be apparent over a much larger time intervale.

A qualitative examination of the experimental time dependences of $\langle R\rangle(t)$ and $n(t)$ for long annealing times (Fig. 4) suggests that Ag nanocrystals are growing by coarsening. In order to compare quantitatively our experimental results with the predictions of LSW theory, $\langle R\rangle^3$ and n^{-1} were plotted as functions of the annealing time in Fig. 5. The linear dependences of both experimental functions agree with LSW theory [Eqs. (2) and (3), respectively]. As expected, the slope of $\langle R\rangle^3$ and n^{-1} increases for increasing temperatures. Due to the very small variation in the total precipitated volume fraction during the coarsening process, a detailed quantitative comparison of the experimental function $\varphi(t)$ with the time dependence predicted by Eq. (5) was not attempted.

Since γ, c_i, and c_e are not known for the nanocomposite studied here, a connection between the theoretical values expected for the rate parameters [angular coefficients of Eqs. (2) and (3)] and the slope of the experimental curves plotted in Fig. 5 was not tried. However, we could determine, as will be described below, the activation energy for diffusion of Ag atoms in the sodium borate glass.

Assuming that γ, ν, and c_e are temperature independent, the equation relying on the diffusion coefficient and the rate parameter of Eq. (2), κ, can be written as

$$D(T) \propto \kappa(T)T, \tag{9}$$

where $\kappa(T)=8\gamma\nu^2c_eD/(9kT)$ is determined from the slope of the straight lines in Fig. 5(a). On the other hand, the Arrhenius equation predicts that $D(T)$ is proportional to

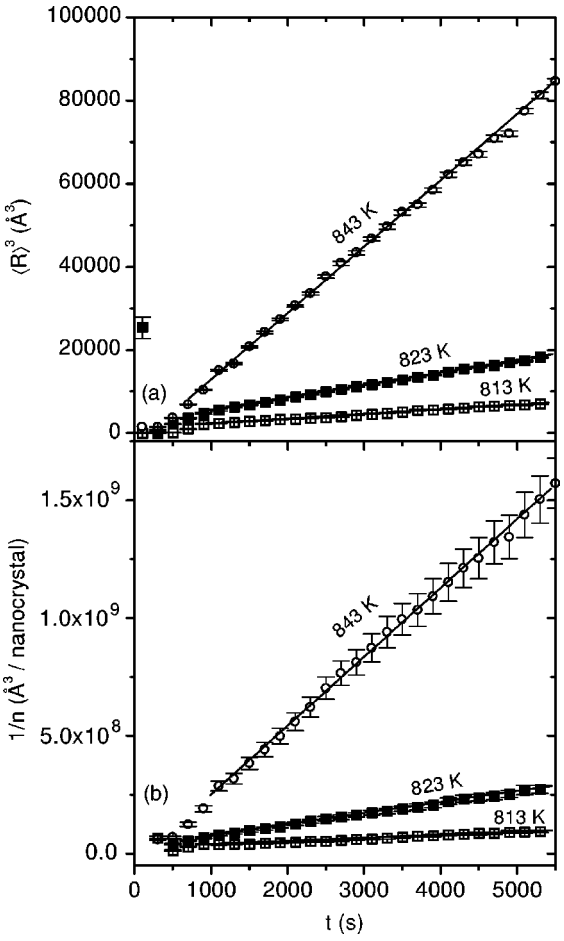

FIG. 5. (a) Cubic average radius $\langle R\rangle^3(t)$ and (b) inverse of Ag nanocrystals number density $n^{-1}(t)$ for different annealing temperatures. The linear dependences observed in these plots, at advanced stages, are in agreement with those predicted by the LSW theory. The straight lines correspond to linear regressions of experimental data.

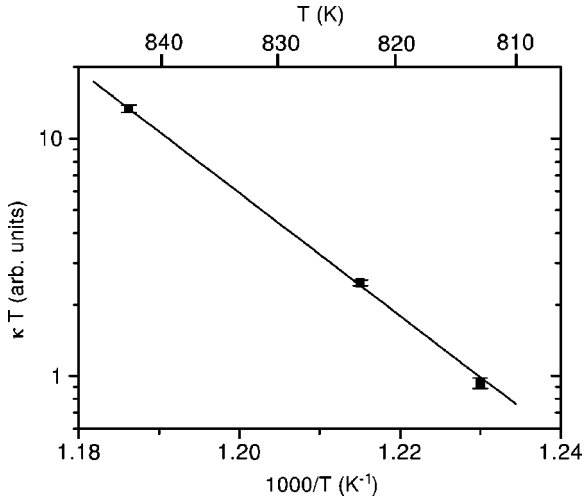

FIG. 6. $\kappa T(\propto D)$ as a function of the inverse of the temperature $1/T$. From the slope in the log $\kappa\ T\times 1/T$ plot the activation energy of the diffusion process was determined.

$\exp(-E/\Re T)$, where E is the activation energy for the diffusion process and $\Re$ is the gas constant. So as according to Eq. (9) the following equation holds:

$$\kappa(T)T \propto e^{-E/(\Re T)}. \tag{10}$$

It should be noted that the assumption regarding γ, ν, and c_e is reasonable because the diffusion coefficient exhibits a much stronger and dominant variation with temperature.

The results plotted in Fig. 6 illustrate the actual validity of Eq. (10). From the slope of the straight line in the $\log(\kappa T)\times 1/T$ plot (Fig. 6) the value of the activation energy for Ag diffusion through the glass, $E=(49\pm 1)\times 10^4$ J mol^{-1}, was obtained. This activation energy is slightly smaller than that obtained for the diffusion of Bi atoms in the same matrix $[(64\pm 3)\times 10^4$ J mol$^{-1}]$.[18]

The relative radius dispersions, σ_R, as functions of the annealing time for different temperatures are displayed in Fig. 4(d). The large radius dispersion for short annealing times is explained as being a consequence of a continuous nucleation of new clusters along the isothermal annealing. The continuous diminution of Ag concentration in the glass matrix reduces the nucleation rate and σ_R falls to a minimum. After this initial nucleation and growth stage, σ_R increases very slightly and, at advanced stages, it becomes nearly constant.

At advanced stages of coarsening at 843 K, σ_R is equal to 0.21 in agreement with the prediction of LSW theory. However, for glasses annealed at 823 and 813 K the asymptotic values of σ_R are lower, namely 0.17 and 0.14, respectively. The observed reduction of σ_R for decreasing temperatures is not at present fully understood. Probably, this effect is a consequence of a possible contribution of elastic strains resulting from the cluster formation in the glass annealed at 813 and 823 K, this contribution being not so important at $T=843$ K. In this regard, it was demonstrated by Schmelzer and Möller[13] that, when the mobility of the matrix building units is much lower than that of the precipitating atoms, the asymptotic behavior in coarsening regime is modified, this effect leading to a significant reduction in the size dispersion. This finding suggests that the elastic strain increases for decreasing temperatures leading to a reduction in clusters size dispersion. Our experimental results are in accordance with this theoretical consideration. On the other hand, we have observed that at the highest annealing temperature ($T=843$ K) the glass sample exhibits a noticeable macroscopic flow. This indicates that, at this temperature, the viscosity is rather low—the atomic mobility is high—and, consequently, elastic strains do not develop. Thus, as experimentally observed, only for $T=843$ K, σ_R is expected to be in accordance with the value (0.21) predicted by the LSW theory for strain free systems.

V. CONCLUSION

The reported SAXS results—regarding the phase separation and nanocrystal formation in supersaturated Ag-doped sodium borate glass—indicate that Ag nanocrystals are formed from the very beginning of the process, i.e., during

the quenching from the liquid down to room temperature. Subsequently, after a few minutes of isothermal annealing, a second population of a large number of small nanocrystals starts to nucleate.

The whole phase separation process involves three distinct stages: (i) a short incubation period, (ii) the nucleation and growth of small Ag crystals driven by diffusion through the glass matrix and further aggregation of isolated Ag atoms, and (iii) a final and rather slow coarsening process during which the Ag concentration in the matrix is close to the equilibrium value and the large nanocrystals still grow at the expense of the small ones.

During the advanced—coarsening—stage, the time dependence of the average radius and density number of Ag nanocrystals, derived from our SAXS results, agree with the predictions of the LSW model. On the other hand, the relative radius dispersion obtained from the radius distribution are nearly time invariant for all annealing temperatures. For the highest annealing temperature ($T=843$ K), the relative radius dispersion obtained from SAXS experiments agrees with that predicted by the LSW theory. However, for lower annealing temperatures, the relative radius dispersion is noticeably smaller than theoretically expected, this deviation probably being an effect coming from strains developed during the annealing processes.

From the time dependence of the nanocrystals average radius $\langle R\rangle(t)$, at different annealing temperatures, the activation energy involved in the Ag diffusion through the glass matrix was quantitatively determined, this value been equal to $E=(49\pm1)\times10^4$ J mol^{-1}.

It was also verified that the Ag nanocrystal radius distribution is better described by a log-normal function than by the function derived from the LSW model. This same conclusion was already reported by several authors that studied similar systems, but this finding was not up to now clearly understood. In order to clarify this issue, further theoretical investigation is required.

ACKNOWLEDGMENTS

The authors thank L. C. Barbosa for helpful suggestions for sample preparation. This work was supported by LNLS and by PRONEX/CNPq and FAPESP (Brazilian funding agencies).

*Author to whom correspondence should be addressed. Permanent address: Laboratório Nacional de Luz Síncrotron, C.P. 6192, 13084-971 Campinas SP, Brazil. Email address: keller@lnls.br

[1] F. Gonella and P. Mazzoldi, *Handbook of Nanostructured Materials and Nanotechnology* (Academic, New York, 2000).
[2] H. Itoigawa, T. Kamiyama, and Y. Nakamura, J. Non-Cryst. Solids **220**, 210 (1997).
[3] G. Kellermann, A. F. Craievich, R. Neuenschwander, and T. S. Plivelic, Nucl. Instrum. Methods Phys. Res. B **199**, 112 (2003).
[4] G. Kellermann, F. Vicentin, E. Tamura, M. Rocha, H. Tolentino, A. Barbosa, A. F. Craievich, and I. L. Torriani, J. Appl. Crystallogr. **30**, 880 (1997).
[5] D. Orthaber, A. Bergmann, and O. Glatter, J. Appl. Crystallogr. **33**, 218 (2000).
[6] I. M. Lifshitz and V. V. Slyozov, J. Phys. Chem. Solids **19**, 35 (1961).
[7] C. Wagner, Z. Elektrochem. **4**, 581 (1961).
[8] J. Schmelzer, I. Gutzow, and R. Pascova, J. Cryst. Growth **104**, 505 (1990).
[9] A. J. Ardell, *Proceedings of the International Conference on Mechanism of Phase Transformation in Crystalline Solids, London, 1969*, Report No. 33 (The Institute of Metals, London, 1969), p. 111.
[10] P. W. Voorhees, J. Stat. Phys. **38**, 231 (1985).
[11] P. W. Voorhees, Annu. Rev. Mater. Sci. **22**, 197 (1992).
[12] A. J. Ardell, in *Phase Transformations '87* (Institute of Metals, London, 1988), p. 485.
[13] J. Schmelzer and J. Möller, Phase Transitions **38**, 261 (1992).
[14] O. Glatter and O. Kratky, *Small Angle X-ray Scattering* (Academic, London, 1982).
[15] J. W. Christian, *The Theory of Transformations in Metals and Alloys* (Pergamon, New York, 1975).
[16] L.-C. Liu and S. H. Risbud, J. Appl. Phys. **76**, 4576 (1994).
[17] P. Staron, B. Jamnig, H. Leitner, R. Ebner, and H. Clemens, J. Appl. Crystallogr. **36**, 415 (2003).
[18] G. Kellermann and A. F. Craievich, Phys. Rev. B **67**, 085405 (2003).
[19] J. Bartels, U. Lembke, R. Pascova, J. Schmelzer, and I. Gutzow, J. Non-Cryst. Solids **136**, 181 (1991).
[20] M. Haselhoff and H.-J. Weber, Phys. Rev. B **58**, 5052 (1998).
[21] A. J. Ardell and R. B. Nicholson, J. Phys. Chem. Solids **27**, 1793 (1966).
[22] G. Oskam, Z. Hu, R. L. Penn, N. Pesika, and P. C. Searson, Phys. Rev. E **66**, 011403 (2002).